Molecular imaging of tumor-associated macrophages in cancer immunotherapy

Xiaoying Li (ID), **Ruike Wang, Yangnan Zhang, Shuangze Han, Yu Gan, Qi Liang, Xiaoqian Ma, Pengfei Rong, Wei Wang and Wei Li** (ID)

Abstract: Tumor-associated macrophages (TAMs), the most abundant inflammatory cell group in the tumor microenvironment, play an essential role in tumor immune regulation. The infiltration degree of TAMs in the tumor microenvironment is closely related to tumor growth and metastasis, and TAMs have become a promising target in tumor immunotherapy. Molecular imaging is a new interdisciplinary subject that combines medical imaging technology with molecular biology, nuclear medicine, radiation medicine, and computer science. The latest progress in molecular imaging allows the biological processes of cells to be visualized *in vivo*, which makes it possible to better understand the density and distribution of macrophages in the tumor microenvironment. This review mainly discusses the application of targeting TAM in tumor immunotherapy and the imaging characteristics and progress of targeting TAM molecular probes using various imaging techniques.

Keywords: cancer, immunotherapy, molecular imaging, tumor-associated macrophages

Introduction

Molecular imaging combines the characteristics of molecular biology technology and modern medical imaging with fluorescence tools, and small molecules and metals can be illuminated to observe the biological processes of cells and sub-cells *in vivo*.[1,2] Compared with traditional imaging techniques, the advantages of molecular imaging can be summarized as follows: (1) turn complex biological processes (gene expression and biological signal transduction) into intuitive visual images, (2) detect early molecular variations and pathological changes in cells before anatomical changes of the disease, (3) assess the therapeutic response early by measuring changes in the expression of molecular targets, and (4) measure the biological distribution of drugs *in vivo*.[3] The joint development of medical imaging instruments and imaging materials (such as contrast agents, molecular probes, and reporter genes) has promoted molecular imaging in clinical applications. The existing imaging techniques include positron emission tomography (PET), single-photon emission computed tomography (SPECT), magnetic resonance imaging (MRI), computed tomography (CT), ultrasound (US),

optica imaging, and emerging techniques such as hyperpolarized MRI, magnetic particle imaging (MPI), and photoacoustic imaging (PAI).[4,5] At present, molecular imaging technology is widely used in studies on oncology,[6] cardiovascular diseases,[7] and the nervous system[8] and has achieved some breakthroughs in disease diagnosis, treatment, and curative effect evaluations.

In recent years, the role of the tumor microenvironment (TME) in cancer progression and metastasis has garnered much interest. New targeted therapies are now focused on tumor cells themselves and on disrupting the interactions between tumor and stromal cells.[9] Inhibitors targeting immune checkpoints (ICs), such as anti-PD-1/L1 and anti-CTLA-4 monoclonal antibodies (mAbs), have been used to treat non-small cell lung cancer,[10] melanoma,[11] and breast cancer.[12] Tumor-infiltrating lymphocytes (TILs)[13] and macrophages[14] have also been studied in preclinical or clinical trials.

Tumor-associated macrophages (TAMs) play particular functionals in tumor progression, including cancer initiation and promotion,

Correspondence to:
Pengfei Rong
Department of Radiology,
The Third Xiangya
Hospital of Central South
University, Changsha
410013, Hunan, People's
Republic of China.
rongpengfei66@163.com

Cell Transplantation and
Gene Therapy Institute,
The Third Xiangya
Hospital, Central South
University, Changsha,
People's Republic of China

Wei Wang
Department of Radiology,
The Third Xiangya
Hospital of Central South
University, Changsha
410013, Hunan, People's
Republic of China.
cjr.wangwei@vip.163.com

Cell Transplantation and
Gene Therapy Institute,
The Third Xiangya
Hospital, Central South
University, Changsha,
People's Republic of China

Wei Li
Department of Radiology,
The Third Xiangya
Hospital of Central South
University, Changsha
410013, Hunan, People's
Republic of China.
weililx@csu.edu.cn

Cell Transplantation and
Gene Therapy Institute,
The Third Xiangya
Hospital, Central South
University, Changsha,
People's Republic of China

**Xiaoying Li
Ruike Wang
Yangnan Zhang
Shuangze Han
Yu Gan
Qi Liang
Xiaoqian Ma**
Department of Radiology,
The Third Xiangya
Hospital of Central South
University, Changsha,
People's Republic of China

Cell Transplantation and
Gene Therapy Institute,
The Third Xiangya
Hospital, Central South
University, Changsha,
People's Republic of China

local immunosuppression, metastasis, and drug resistance.[15,16] At present, targeted TAM immunotherapy in (pre)clinical applications is mainly focused on decreasing the TAM population, promoting macrophage phagocytic activity, and reprogramming TAMs to an antitumor M1 type. There is an urgent need for methods that can be used to evaluate the presence, subtypes, and density of macrophages in the TME. The gold standard for assessing macrophages in tumor tissues is immunohistochemistry (IHC), flow cytometry, or gene expression analysis. These techniques can provide detailed molecular and morphological information. However, they require the sacrifice of animals and cannot be used when biopsy samples are not available. The development of molecular imaging provides a starting point for solving these problems. Optical imaging, PET/SPECT, MRI, and US have been used to track and monitor the dynamic changes in TAMs noninvasively. Individual or combined use of these imaging strategies might help stratify patients before or during the early stages of immunotherapy.[17] This review mainly discusses the application of TAM-based tumor immunotherapy and highlights the latest advances in molecular imaging technology for macrophage tracking.

TAMs in cancer immunotherapy

TAMs represent the main immune cell population of the TME and have been mainly classified into the antitumor type M1 phenotype (classically activated state) and the protumor M2 phenotype (alternatively activated state).[18] In terms of protein expression, M1 macrophages are characterized by the expression of proinflammatory cytokines (tumor necrosis factor alpha, TNF-α; interleukin 6, IL-6; or interleukin 12, IL-12), major histocompatibility complex (MHC) molecules, and inducible nitric oxide synthase (iNOS). M2 macrophages decrease the expression of these molecules and recognize various landmarks such as Arg1, mannose receptor, and scavenger receptor.[19] Macrophages are plastic cells that can adopt different phenotypes depending on the immune context. Under the stimulation of CSF-1 (colony-stimulating factor-1), interleukin 10 (IL-10), or interleukin 13 (IL-13), macrophages differentiate into M2 phenotype, which promotes tumor development mainly through the following points: (1) suppress tumor immunity by (i) secreting effector molecules (IL-10, ARG1, indoleamine 2, 3-dioxygenase (IDO) and transforming growth factor-β (TGF-β), (ii) expressing inhibitory receptors (MHC-I, PD-L1, and CD86) to reduce the

activities of T cells and natural killer (NK) cells, or (iii) secreting chemokines CCL5, CCL22, and CCL20 to recruit immune suppressive cells[20]; (2) promotes tumor angiogenesis by producing pro-angiogenic cytokines and growth factors such as vascular endothelial growth factor (VEGF), platelet-derived growth factor (PDGF), angiopoietin 2, CXCL1, and FGF-2[21]; and (3) promotes tumor cell invasion and metastasis by (i) releasing effector molecular cathepsin, MMP2, MMP9, CCL18, and CYP4A, which are involved in extracellular matrix (ECM) destruction,[22] (ii) various factors such as TNF-α, epidermal growth factor (EGF), CCL18, osteonectin, and cathepsin are able to promote tumor cell intravasation,[23] and (iii) chemokines and cytokines of CXCL8,[24] CSF-2, TNF-α, ICAM-1, and IL-6[25] contribute to epithelial-mesenchymal transition (EMT). In contrast, lipopolysaccharide (LPS) and interferon-gamma (INF-γ) induced macrophages to differentiate into the M1 phenotype, which has the antitumor activity of scavenging and destroying phagocytic tumor cells secreting IL-12, TNF-α, and iNOS and initiating Th1.[26,27]

Increased TAM infiltration correlates with an inert response to cancer treatment and poor prognosis in multiple cancer models.[28] Hence, targeting TAMs is a potential and promising strategy for cancer immunotherapies. Immunotherapeutic strategies fall into three major categories: (1) decreasing the TAM population, (2) promoting macrophage phagocytic activity, and (3) reprogramming TAMs to an antitumor M1 phenotyope (Figure 1). TAM-targeted therapies can also function as combination therapies to promote traditional or IC treatments' antitumor effect.

Decreasing the TAM population

TAMs have mainly two different origins: much greater of them, termed bone marrow–derived macrophages (BDMs), are derived from circulating monocytes and recruited to the tumor site *via* CSF-1, monocyte chemoattractant protein 1 (MCP1), and hypoxic conditions[29]; another is derived from tissue-resident macrophages (TRMs), which maintain themselves through proliferation and limited self-renewal such as in the lungs (alveolar macrophages), brain (microglia), and liver (Kupffer cells).[30] Correspondingly, there are two main approaches to reduce the number of TAMs: limiting macrophage recruitment to tumor tissue and depleting the macrophages already extant in tumor tissue.
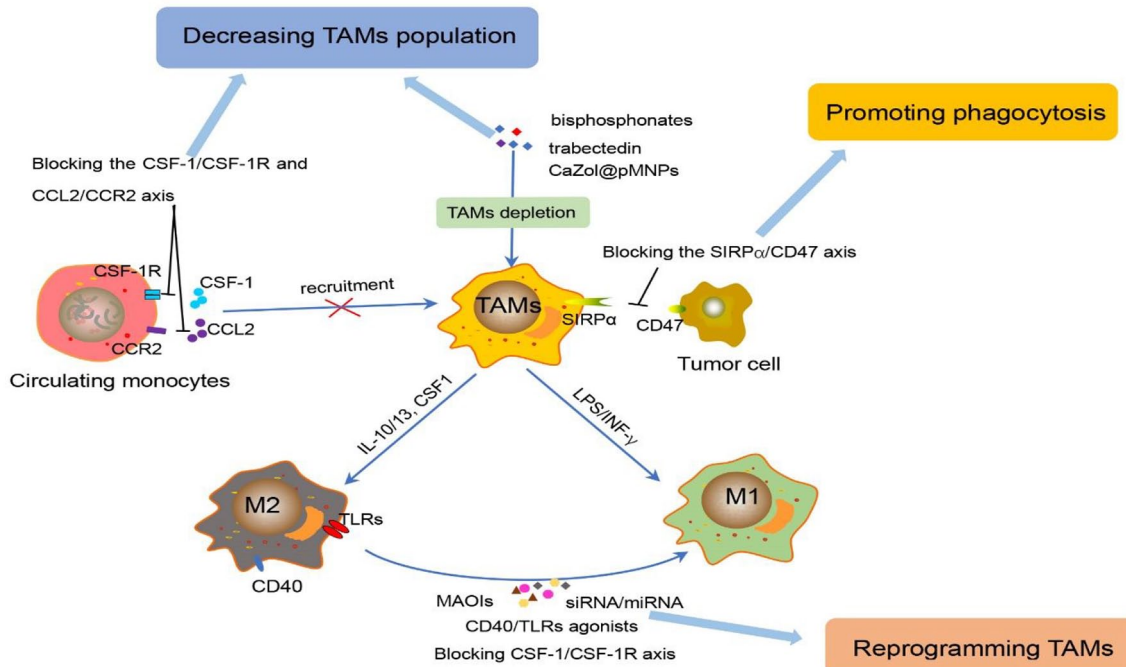
Figure 1. Immunotherapeutic strategies of targeting TAMs. The immunotherapeutic strategies fall into three main points: (1) decreasing the TAM population by blocking the CSF-1/CSF-1R axis and CCL2/CCR2 axis to inhibit the monocyte recruitment, and depleting TAMs with drugs (bisphosphonates, trabectedin, and CaZol@ pMNPs) to induce their apoptosis; (2) promoting macrophage phagocytic activity by blocking the SIRFα/CD47 axis; and (3) reprogramming TAMs to an antitumor M1 by CD40/TLR agonists, siRNA/miRNA, and MAOIs, and blocking CSF-1/CSF-1R axis.
CCL2/CCR2, C–C chemokine ligand 2/C–C chemokine receptor 2; CSF-1/CSF-1R, colony-stimulating factor-1/colony-stimulating factor-1 receptor; IL-10/13, interleukin 10/13; INF-γ, interferon-gamma; LPS, lipopolysaccharide; miRNA, microRNA; siRNA, small interfering RNA; SIRPα, signal regulatory protein alpha; TAMs, tumor-associated macrophages; TLRs, toll-like receptors.

Limiting the recruitment of circulating monocytes into the TME is a promising strategy to reduce protumor TAMs. Some trials targeting chemoattractants secreted by malignant and stromal cells have been investigated such as macrophage CSF-1[31] and C–C motif chemokine ligand 2 (CCL2)[32] and their receptors. CSF-1/CSF-1R (colony-stimulating factor-1 receptor) is critical for monocyte recruitment to the tumor site and differentiation into M2 macrophages. PLX3397 (an inhibitor of CSF-1R) has been found to effectively decrease the number of TAMs and circulating monocytes in mesothelioma mouse models. It can augment survival synergistically, reduce TAMs, and increase the number and function of CD8+ T cells when combined with dendritic cell vaccination.[33] In addition to solid tumors, targeting CSF-1R has been proven effective in hematopoietic malignancies. It has been demonstrated that BLZ945 (CSF-1R inhibition) could block leukemia-associated monocyte-derived cell (LAM)

polarization and deplete LAMs in a mouse model of T-cell acute lymphoblastic leukaemia (T-ALL).[34]

CCL2, a chemokine released by monocytes and tumor cells, and its receptor C–C chemokine receptor type 2 (CCR2) play a critical role in mediating monocyte egress from the bone marrow into the TME.[35] Blocking the CCL2/CCR2 axis has effectively reduced tumor growth in several animal models.[36,37] Wang *et al.*[32] found that both CCL2 and CCL5 are indispensable in promoting TAM infiltration and driving polarization toward the M2 phenotype during hepatocellular carcinoma (HCC) progression. Similar results were found in the glioma of CCR2–/– (Ccr2KO) mice. Immunofluorescence staining showed that the number of TAMs in intratumoral areas decreased by approximately 30%, while peritumoral regions were not significantly affected.[38] Recent studies have reported that targeting other

chemikines, CXCL12/CXCR4[39] and Periostin,[40] related to the recruitment of TAMs has been confirmed to have an antitumor effect.

Depleting macrophages already extant in tumor tissue has also shown an antitumor effect. Some compounds, including trabectedin,[41] bisphosphonates,[42] and clodronate liposomes,[43] have been confirmed to scavenge TAMs by inducing their apoptosis effectively. Lipid-coated calcium zoledronate-encapsulated complexes (CaZol@pMNPs) were developed and conjugated to mannose, which was used to target TAMs and specifically enhance the cytotoxicity of macrophages. *In vivo* and *in vitro* experiments showed that it could specifically aggregate in tumor tissues and deplete TAMs, and the expression of IL-10, VEGF, and MMP9 decreased significantly.[44] A recent report constructed a group of bi- and tri-valent T-cell engagers (BiTEs/TriTEs) that can preferentially recognize CD3 ε on T cells and CD206 or folate receptor β (FR-β) on M2-like macrophages to kill M2-polarized macrophages over M1-polarized macrophages. This study achieved selective depletion of specific M2-like macrophage subsets for the first time.[45]

Promoting macrophage phagocytic activity

The successful growth and maturation of tumors need to evade all kinds of immune surveillance activities effectively, for example, to escape the phagocytosis of macrophages. One key mechanism of tumor cell immune escape is through upregulation of the immunosuppressive signaling molecule CD47, which interacts with signal regulatory protein alpha (SIRPα) on macrophages to transmit the 'don't eat me' signal.[46] Blocking the CD47-SIRPα axis is an exciting strategy to enhance TAM phagocytic properties. Several CD47-SIRPα blocking agents have been developed such as fully human anti-CD47 antibodies, anti-CD47 single-chain variable fragments, anti-SIRPα antibodies, and high-affinity monomeric SIRPα devoid of the Fc portion.[47] In *in vitro* and preclinical studies, these agents have shown antitumor effects on multiple tumor types, and some of them are now being tested in clinical trials,[48] for example, the agents TTI-621 (SIRPαFc)[49] and Hu5 F9-G4 (5F9).[50] However, recent reports suggest that blockade of CD47-SIRPα signaling in isolation is insufficient and might be associated with toxic reactions such as transient anemia, fatigue, and headache.[51] Apart from this strategy, some studies have found that interleukin 5 (IL-5),

granulocyte-macrophage colony-stimulating factor (GM-CSF),[52] and PBI1 – a toll-like receptor (TLR) agonist[53] – can also stimulate macrophages to enhance phagocytic activity.

Reprogramming TAMs to antitumor M1 phenotyope

In light of this characteristic plasticity, reprogramming TAMs to antitumor M1 is an ideal strategy for cancer immunotherapy, including TLR agonists,[54] blockade of the CSF-1/CSF-1R axis,[55] interference RNAs – small interfering RNA (siRNA) or microRNA (miRNA),[56] monoamine oxidase inhibitors (MAOIs),[57] and CD40 agonists.[58]

As a type of pathogen pattern recognition receptor (PRR), TLRs are innate immunity PRRs expressed by antigen-presenting cells (APCs), including macrophages. The activation of TLRs can induce the immune response, reprogramming TAMs to the M1 phenotype, which has been proven in preclinical or clinical trials with TLR3, TLR7, TLR8, and TLR9 agonists in many tumor models.[54,59] Recently, to better target macrophages and reduce side effects, TLR agonists such as CpG oligodeoxynucleotides (CpG ODNs) have been targeted for delivery with the nanoparticle vector murine M2 macrophage-targeting peptide M2pep. In four T1 tumor-bearing mice, these M2pep-rHF-CpG nanoparticles repolarized M2 TAMs to the M1 type and inhibited tumor growth after intravenous injection.[60]

miRNAs have been demonstrated to participate in myeloid differentiation and macrophage activation in previous studies by suppressing the expression of target genes.[61] In orthotopic HCC or subcutaneous Lewis lung cancer (LLC) mice, miR-99b and/or miR-125a were delivered into TAMs, and the authors found that miR-99b or miR-125 treatment increased the expression of M1 markers (such as IL-6, TNF-α, and iNOS) while decreasing the M2-specific marker Arg1, which contributed to inhibiting tumor growth.[56]

Monoamine oxidase A (MAO-A) is an enzyme best known for its function in the brain, and correlation studies of clinical data show that high intratumoral MAO-A expression in a wide range of cancers is associated with poor patient survival. Sikic *et al.* demonstrated that the tumor-promoting effect of MAO-A is related to the promotion of TAM immunosuppressive polarization. They found that tumor growth in MAO-A knockout

(KO) mice was significantly suppressed than MAO-A wild-type (WT) mice. The TAMs in the former exhibited a less immunosuppressive phenotype, with low expression of immunosuppressive molecules (CD206), while the expression of immunostimulatory markers (CD86, CD69) increased.[57]

The Cluster of Differentiation 40 (CD40) is a member of the tumor necrosis factor (TNF) receptor family and is widely expressed by tumor cells and APCs. Studies have found that treatment with CD40 agonists alone or with anti-CSF-1R antibodies in preclinical tumor models can decrease immunosuppressive macrophages and increase maturation and differentiation of proinflammatory TAMs.[62] Two agonistic anti-CD40 antibodies (CP-870,893 and RO7009789) are being tested in clinical trials. CP-870,893 was administered in combination with gemcitabine chemotherapy in a phase I trial for patients with pancreatic cancer; the results showed it was well tolerated, and partial responses (PRs) were identified in approximately 20% of patients.[63]

Overview on molecular imaging

Molecular imaging is a technique based on radionuclides or optical probes to observe tumor biomarkers in real time and accurately monitor the dynamic changes in target genes.[64] Among the imaging modalities, each technique has its inherent strengths and weaknesses (Table 1). PET/SPECT, a radionuclide-based molecular imaging technology, is used extensively in preclinical and clinical researches due to its high sensitivity and total body penetrance. It can realize the early diagnosis, treatment guidance, and study of the molecular mechanisms of diseases *via* evaluating the molecular changes in the physiological and biochemical processes of the human body by using the appropriate radiolabled-imaging agents.[65] However, PET and SPECT are limited by spatial resolution and examination cost.[66] MRI has the characteristics of high-resolution soft tissue and three-dimensional multiparameter imaging. It can effectively detect and diagnose the disease by combining with contrast agents. Compared with other molecular imaging modalities, low sensitivity for molecular detection is the major shortcoming.[67] Optical imaging mainly includes bioluminescence imaging (BLI) and fluorescence imaging (FLI). The relatively low implementation, high sensitivity, and nonradioactive properties make this noninvasive imaging technique preferred in preclinical research.[68] At present, tissue penetration and image resolution are still a defect of optical imaging, leading to its not being entered into clinical application. US imaging, a versatile and mature diagnostic technique widely used in human and veterinary medicine, uses the interaction between sound waves and living tissue to produce images or to measure the velocity of tissue movement (mainly blood) based on Doppler mode. Due to the great influence of gas and high density of bone, its application in the examination of organs such as lungs and intestines is limited.[69] Since each imaging technique has its advantages and disadvantages, particular clinical problems and biological characteristics are the main determinants of imaging technology selection and joint application.

Tracking TAMs by molecular imaging

Taking advantage of the characteristics of these imaging techniques allows us to expand our knowledge of TAM-based immunotherapies and provide bridges to the clinical applications of these therapies. Despite advances in immuneoncology, most patients still exhibit primary or acquired therapeutic resistance mediated by immunosuppressive macrophages.[70] The preclinical and clinical data showed that patients with intense TAM infiltration could benefit from TAMs targeting immunotherapies, highlighting the need for specialized techniques to detect and quantify TAM populations to improve treatment outcomes for cancer patients. Molecular imaging can screen suitable patients, and monitor and evaluate immunotherapeutic efficacy and prognosis.[71] Therefore, molecular imaging is exceedingly helpful in the development of TAM-based immunotherapies. The characteristics of targeting TAM imaging techniques and TAM-labeling strategies are illustrated in Tables 1 and 2. Several specific targets of TAMs for imaging have been demonstrated such as the macrophage mannose receptor (MMR or CD206), translocator protein (TSPO), phagocytic activity, FR-β, CSF-1R, F4/80, TLRs, and SIGN-R1 (specific ICAM-3-grabbing nonintegrin-related 1) (Figure 2(A)).

MMR, CD206

MMR, CD206, is an intracellular C-type lectin receptor. As an immune adhesion molecule,

Table 1. Characteristics of targeting TAM imaging techniques.

Imaging modality	Advantages	Disadvantages	Labeling method	Purpose	Clinical translation	Applied commercially
PET/ SPECT	• High sensitivity • Unlimited penetration depth • Accurate quantitation	• Low spatial resolution • Expensive • Radioactive	^{99m}Tc	Tracking	Yes	Yes
			^{64}Cu	Tracking	Yes	Yes
			^{18}F	Tracking	Yes	Yes
			^{68}Ga	Tracking	Yes	Yes
			^{11}C	Tracking	Yes	Yes
			^{89}Zr	Tracking	Yes	Yes
			^{125}I	Tracking	Yes	Yes
			^{111}In	Tracking	Yes	Yes
MRI	• High spatial resolution • Excellent molecular and anatomical information • No radiation hazard	• Low sensitivity • Long imaging time • Expensive	IONPs (Ferumoxytol)	Tracking and therapy	Yes	Yes
			PFC	Tracking and quantification	Yes	Yes
MPI	• High temporal and spatial resolution sensitivity • High sensitivity • No radiation hazard • Quantitation	• Human-sized MPI scanners are not available • Few tracers	IONPs (Ferumoxytol or Ferucarbotran)	Tracking and quantification	Limited	Yes
FLI	• Fast acquisition • Easy dye labeling • No radiation hazard • High sensitivity • Low cost	• Poor tissue penetration • Low spatial resolution	IRDye700	Tracking and therapy	Limited	Yes
			NIR dye Cy7	Tracking	Limited	Yes
			NIR dye	Tracking	Limited	Yes
			DN-ICG	Tracking	Limited	Yes
			ZW800-1C	Tracking	Limited	Yes
US	• Good temporal resolution • Low cost • No radiation hazard	• Limited examination of skeletal and hollow organs • Rely on the operator's technical level	HA-FOL-NBs	Tracking and therapy	Yes	No
			NB_{CSF-1R}	Tracking	Yes	No

CSF-1R, colony-stimulating factor–1 receptor; DN-ICG, dextran-indocyanine green; FLI, fluorescence imaging; HA-FOL-NBs, hyaluronic acid folate-conjugated nanobubbles; IONPs, iron oxide nanoparticles; MPI, magnetic particle imaging; MRI, magnetic resonance imaging; NB, nanobubble; NIR, near-infrared; PET, positron emission tomography; PFC, perfluorocarbon compound; SPECT, single-photon emission computed tomography; TAM, tumor-associated macrophage; US, ultrasound.

Table 2. Molecular imaging strategies for TAM tracking.

Target	Type of imaging	Tracer	Tumor model	Duration of tracking	Results	References
MMR	PET	99mTc-labeled anti-MMR nanobodies	TS/A (mammary carcinoma), 3LL-R (lung carcinoma)	1–3h	Specifically labeled MMR+ TAMs, and substantial uptake in the tumors, spleen, and liver	Movahedi et al.[72]
	PET	64Cu-labeled MAN-LIPs	Mouse lung carcinoma	6h	High uptake in lung tumors at 6-h post-injection and rapid clearance in normal lung	Locke et al.[73]
	PET	[99mTc]-anti-MMR-sdAb, [18F]FB-anti-MMR-sdAb	3LL-R (lung carcinoma)	1–3h	Imaging showed the highest signal was present in the tumor and MMR-expressing organs such as the liver, spleen, and lung	Blykers et al.[74]
	SPECT/NIRF	125I-αCD206/Dye-αCD206	4T1 (breast cancer)	24h/4–96h	The probe markedly increased accumulation in relapse-prone tumors at 24 h after injection, and uptake of this radiotracer in tumor-draining lymph nodes was higher	Zhang et al.[75]
	PET/CT	[68Ga]Ga-NOTA-anti-MMR-sdAb	3LL-R (lung carcinoma)	1–2.5h	High-specific uptake in MMR-expressing TAMs and organs, with no observed toxicity	Xavier et al.[76]
	NIRF/SPECT	IRD-αCD206/125I-αCD206	4T1 (breast cancer)	4–24h	The uptake of IRD-αCD206 in the sorafenib-treated tumors was significantly higher	Zhang et al.[77]
	NIRF	Cy7-DM	SMMC-7721 hepatoma tumor	5min–8h	Uptake in stomach, lung, spleen, and especially in tumor with abundant TAMs	Jiang et al.[78]
	NIRF	Dye-anti-CD206	4T1 (breast cancer)	2–48h	Uptake in liver, stomach, and tumor, and can dynamically monitor CD206 expression during anti-macrophage therapy using zoledronic acid	Sun et al.[79]
	MRI	PEG-b-AGE-coated IONPs	4T1 (mouse mammary tumor)	48h	Significantly larger IONP-induced decrease of transverse relaxation time (T2) in tumors attributed to MMR-expressing M2 presence	Li et al.[80]
TSPO	PET	[18F]DPA-714	Gliomas (human cell lines)	0.5–1h	Imaging shows that the tracer signal in the ipsilateral (tumor-bearing) brain hemisphere gradually increases over time, and longitudinal TSPO-PET imaging allows visualizing tumor growth and infiltration	Pigeon et al.[81]
	PET	[18F]DPA-714	Patients with gliomas	1h	Uptake increased in patients with increased infiltration of TSPO-positive CD68+ myeloid cells	Zinnhardt et al.[82]
	PET	[18F]PBR06	Gliomas (human cell lines)	35min	Intense uptake within the tumor implanted in the striatum of the right hemisphere	Buck et al.[83]
	PET	18F-GE-180	Patients with gliomas	1–1.5h	High uptake in tumor and had extraordinarily high tumor-to-background contrast	Albert et al.[84]
	PET	18F-GE-180	Patients with gliomas	60–80min	Uptake in the tumor is closely related to the histological WHO grades and the IDH mutation status	Unterrainer et al.[85]

(Continued)

Table 2. (Continued)

Target	Type of imaging	Tracer	Tumor model	Duration of tracking	Results	References
	PET	[¹¹C]PBR28	Pancreatic cancer	1 h	Significantly uptake in lung, spleen, kidney, and pancreatic cancer with abundant macrophages	Lanfranca et al.[86]
	PET/NIRF	[¹⁸F]V-1008/V-1520	Pancreatic cancer	1 h	Robust uptake in early pancreatic cancer tissue rather than in the surrounding normal tissue	Cohen et al.[87]
Phagocytic activity	MRI	Ferumoxytol	MMTV-PyMT mice (mammary adenocarcinomas)	24 h	Nanoparticles are preferentially phagocytosed by TAMs but not by tumor cells, and tumors show a persistent signal decline at 24-h injection of ferumoxytol	Daldrup-Link et al.[88]
	MRI	Ferumoxytol	Patients with lymphomas and bone sarcomas	24–48 h	Significantly MRI negative (dark) enhancement in TAM-rich tumors, and T2* values correlated significantly with the density of CD68+ and CD163+ TAM	Aghighi et al.[89]
	MPI	Ferumoxytol and Ferucarbotran	4T1 (breast cancer)	24 h	The high signal was visualized in the livers and tumors; it provides quantitative information on the iron labeling of macrophages	Makela et al.[90]
	MRI	PFC	4T1 (breast cancer)	24 h	¹⁹F signal was detected in primary tumors and lung metastases	Makela et al.[91]
	MRI	PFC	Head and neck tumors (human cell lines)	2–10 days	¹⁹F signal is displayed in the periphery of the tumors and the adjacent lymph nodes; it is correlated to the number of macrophages per tumor	Khurana et al.[92]
	PET	⁶⁴Cu-labeled polyglucose nanoparticle (Macrin)	Colon adenocarcinoma, 4T1 (breast cancer), lung adenocarcinoma	24 h	Taking up by TAM selectivity and expressing high signal in tumor areas for PET imaging	Kim et al.[93]
	PET	⁸⁹Zr-HDL	4T1 (breast cancer)	24 h	Strongly uptake in liver, kidney, and tumor (a high degree of macrophage-rich areas)	Perez-Medina et al.[94]
SIGN-R1	NIRF	DN-ICG nanoprobes	Pancreatic cancer	3–24 h	The liver, spleen, and tumor sites have high fluorescence signals, and it can label TAMs with high sensitivity and specificity	Luo et al.[95]
TLRs	NIRF	TLR4-ZW800	HCC	1–48 h	Signals were mainly located in the liver, spleen, kidneys, and TAM-enriched HCC	Ji et al.[96]
FR-β	US	HA-FOL-NBs	Lung carcinoma	0–0.5 h	Specifically target FR-expression TAMs, and reprogram TAM phenotypes from M2 to M1	Sun et al.[97]
F4/80	SPECT	¹¹¹In-anti-F4/80-A3-1	Breast cancer (human cell lines)	24 h	It can visualize TAMs and macrophages in liver and spleen as well	Terry et al.[98]
CSF-1R	US	NB$_{CSF\text{-}1R}$	HCC (human cell lines)	0–0.5 h	The intensity of echo signal around the tumor of HCC was significantly higher than that in the central tissue, which was consistent with the density of TAMs	Jiang et al.[99]

CSF-1R, colony-stimulating factor-1 receptor; CT, computed tomography; DM, deoxymannose; DN-ICG, dextran-indocyanine green; DPA, [N,N-diethyl-2-(2-(4-(2-fluoroethoxy)phenyl)-5,7-dimethylpyrazolo[1,5-a]pyrimidin-3-yl)acetamide; FB, fluorobenzoate; FR-β, folate receptor β; HA-FOL-NBs, hyaluronic acid folate-conjugated nanobubbles; HCC, hepatocellular carcinoma; IONPs, iron oxide nanoparticles; MAN-LIPs, mannosylated liposome; MMR, macrophage mannose receptor; MPI, magnetic particle imaging; MMTV-PyMT, the mammary specific polyomavirus middle T antigen overexpression mouse model; MRI, magnetic resonance imaging; NB, nanobubble; NIRF, near-infrared fluorescence; PET, positron emission tomography; PFC, perfluorocarbon compound; SIGN-R1, specific ICAM-3-grabbing nonintegrin-related 1; SPECT, single-photon emission computed tomography; TAM, tumor-associated macrophage; TLRs, toll-like receptors; TSPO, translocator protein; US, ultrasound; WHO, World Health Organization.
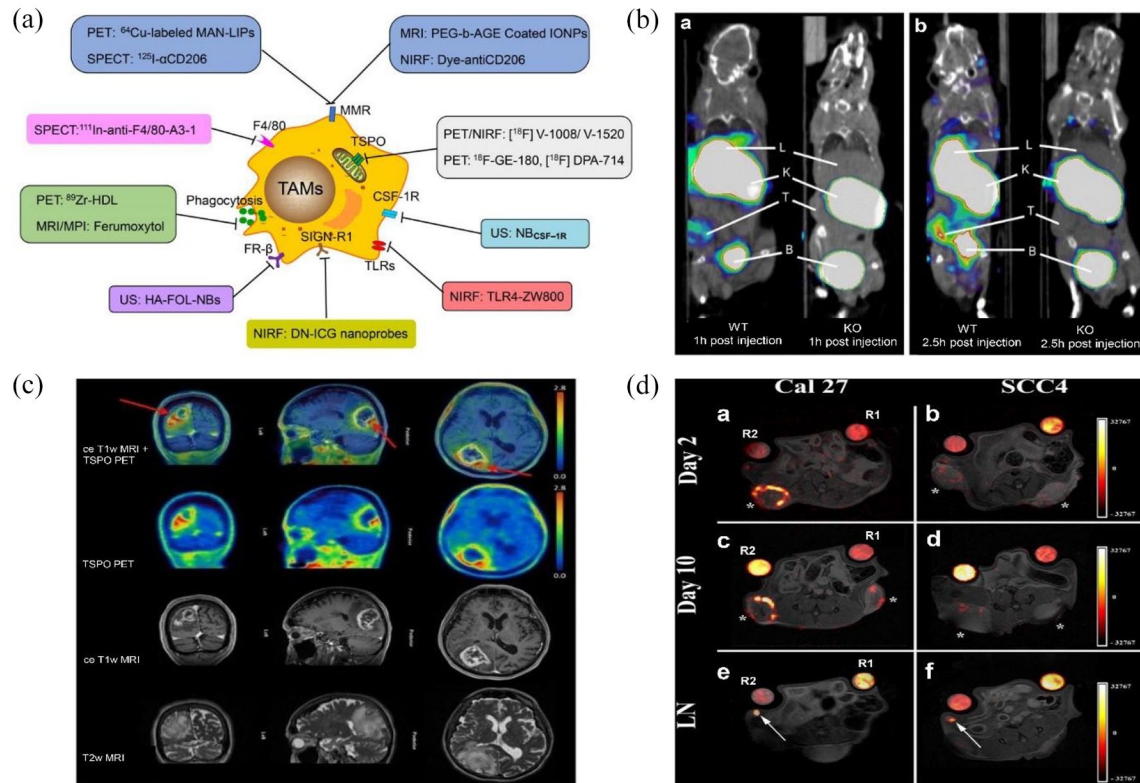
Figure 2. Molecular imaging of TAMs. (A) Some techniques have been applied to target TAM molecular imaging such as PET, SPECT, MRI, US, and optical imaging. The main imaging targets that have been used in clinical or preclinical studies include MMR, TSPO, CSF-1R, TLRs, SIGN-R1, FR-β, F4/80, and its phagocytic activity. (B) Examples of TAM molecular imaging by targeting MMR. Coronal PET/CT images of WT *versus* MMR-deficient (KO) 3LL-R tumor-bearing mice scanned at (a) 1 h and (b) 2.5 h post-injection of [68Ga] Ga-NOTA-anti-MMR-sdAb. Adapted with permission from Xavier *et al.*[76] (C) Examples of TAM molecular imaging by targeting TSPO. TSPO PET in a patient with newly diagnosed glioblastoma in the right occipital lobe. Adapted with permission from Albert *et al.*[84] (D) Examples of TAM molecular imaging by targeting phagocytic activity. *In vivo* MRI displayed PFC distribution in the tumor periphery and draining lymph nodes at days 2 and 10 post-PFC injections. (a, c) 19F signals hotspots of a mouse bearing Cal27 tumors showing significant macrophage infiltrates in the periphery of the tumors. (b, d) 19F signals hotspots of a mouse bearing SCC4 tumors showing decreased macrophage burden. (e, f) fluorine hotspots (arrows) within local LN of the same animals in both Cal27 (e) and SCC4 (f) groups. R1 and R2 indicate tubes for reference quantification, and the color scale is in arbitrary units. Adapted with permission from Khurana *et al.*[92] with minor modifications.
B, bladder; K, kidneys; L, liver; LN, lymph nodes; T, tumors; WT, wild type.

MMR is mainly expressed on the surface of APCs such as specific macrophages and immature dendritic cells.[100] Some studies have shown that MMR is abnormally expressed in various tumors (pancreatic, colorectal, and gastric cancer), and its expression level correlates with the prognosis of patients.[101–103]

Approximately 10 years ago, MMR was confirmed to be a special target for TAM imaging. A report by intravenous injection of 99mTc-labeled anti-MMR nanobodies successfully targeted M2 macrophages *in vivo*. Retention of the nanobody proved to be receptor-specific and absent in MMR-deficient mice.[72] Likewise, Locke *et al.*[73] designed a 64Cu-mannosylated liposome (MAN-LIPs) injected

into a mouse lung cancer model, and *in vivo* PET imaging showed that it mainly accumulated in TAMs and exhibited little accumulation in remote lung areas. Recently, several TAM-targeting tracers binding the MMR have been developed such as [99mTc](CO)3-anti-MMR-sdAb, [18F]FB-anti-MMR-sdAb,[7] 125I-αCD206,[75] and [68Ga]Ga-NOTA-anti-MMR-sdAb.[76] Zhang *et al.* used the tracers of 125I-αCD206 and Dye-αCD206 for SPECT/CT and NIRF (near-infrared fluorescence) imaging demonstrated that they could target CD206 specifically in 4T1 tumors. Furthermore, these methods can noninvasively predict post-chemotherapy tumor relapse and detect metastatic lymph nodes. They chose the four T1 mouse model treated with cyclophosphamide (CTX), and the

result showed that the probe markedly increased accumulation in relapse-prone tumors at 24h after probe injection, and uptake of this radiotracer in tumor-draining lymph nodes was higher than in the control contralateral lymph nodes.[75] Previously, ^{68}Ga-labeled compound for PET/CT imaging of HER2 was found safe and had a low radiation burden on patients in phase I clinical trials.[104] Then, a ^{68}Ga-labeled anti-MMR single-domain antibody (sdAb) fragment was synthesized to assess the presence and density of TAMs. Imaging showed a higher signal in the tumor, liver, and kidneys in WT tumors than in MMR-deficient (KO) tumors (Figure 2(B)). *Ex vivo* evaluation of the bio-distribution confirmed that the specific uptake of this tracer mainly occurs in MMR-expressing tissues (e.g. the liver, spleen, lymph nodes, bone marrow, and tumor).[76]

MMR has also been investigated in optical imaging and MRI. Zhang *et al.*[77] synthesized a probe (IRD-αCD206) targeting sorafenib-resistant tumors and demonstrated that it could be used to visualize TAM recruitment to tumors by NIRF imaging. Cyanine 7 (Cy7) has been widely applied to label and detect proteins, antibodies, and other biological molecules. Jiang *et al.* chose deoxymannose (DM; a high-affinity ligand of mannose receptor) labeled with the near-infrared dye Cy7 to target imaging on TAMs. The results showed that Cy7-DM uptake in the tumor was significantly higher than in other organs and tissues. Moreover, confocal images of tumor tissue show that Cy7-DM staining colocalizes with CD206, indicating the specificity of the probe for M2 macrophages.[78] In a mouse breast cancer model, a DyLight680–antibody conjugate (Dye-antiCD206) was found to allow noninvasive imaging of TAMs *in vivo*. Longitudinal NIRF imaging can be used to reveal the depletion of TAMs in response to zoledronic acid.[79]

Given the inevitable shortcomings of nuclear imaging and optical imaging, to better provide information on the biological dynamics of macrophages, a recent study reports an approach of using anti-biofouling PEG-b-AGE polymer-coated iron oxide nanoparticles (IONPs) to target imaging of MMR-expressing M2-like TAMs. In this case, at 48h after intravenous injection of mannose iron oxide nanoparticles (Man-IONPs) in mice bearing orthotopic four T1 mammary tumors, MRI showed a more significant IONP-induced decrease in transverse relaxation time (T2) in tumors compared with nontargeted IONP

probes. More importantly, this study found no nonspecific uptake cellular of IONPs by M1-like macrophages and cancer cells, and there was no nonspecific interaction between IONPs and serum proteins.[80]

Mannose receptors targeting radiotracers are currently applied to the imaging of macrophages in the TME and proven to have important clinical significance for detecting tumor sentinel lymph nodes,[105] assessing atherosclerotic plaque stability[106] and detecting rheumatoid arthritis early.[107] Hence, MMR is a promising target for the noninvasive detection of macrophages to obtain diagnostic and prognostic information on inflammatory diseases and investigate targeted macrophage immunotherapy.

TSPO

TSPO is an 18-kDa mitochondrial outer membrane protein mainly expressed in activated microglia, astrocytes, and infiltrating macrophages. TSPO has become a promising imaging target in some inflammatory diseases, especially in neuro-inflammatory diseases (such as multiple sclerosis,[108] Parkinson's disease,[109] and glioma).[81]

Different studies have shown that the expression of TSPO is positively correlated with the degree of malignancy and negatively correlated with survival.[110,111] Glioma-associated microglia/macrophages (GAMs) were identified as TSPO sources, and preclinical imaging studies suggested that PET imaging of TSPO could be a potential tool to improve tumor detection and track glioma cell infiltration. The first-generation TSPO radiotracer [11C]PK11195 was successfully used in glioma imaging. However, as a ^{11}C-labeled tracer, [11C]PK11195 has a short half-life and requires a cyclotron to produce the tracer in the field, and a low signal-to-noise ratio limits its use.[112,113] These limitations have led to the development of new TSPO ligands for PET imaging such as [18F]DPA-714,[81,82] [18F]DPA-713,[114] [18F]PBR06,[83] and [18F]GE-180.[84,85] Among the current (pre)clinical tracers used, [18F]DPA-714, a second-generation tracer, has been highlighted as a suitable imaging marker in glioma models.[115,116] Pigeon *et al.* combined diffusion-weighted imaging (DWI) to investigate the potential of [18F]DPA-714 for PET imaging and to assess glioma growth and cell infiltration in a human invasively growing glioma model. This study demonstrated that [18F]DPA-714 PET in combination with DWI may be

superior to conventional imaging methods, such as T2W imaging MRI or [18F]FET PET, in the early detection of tumor and tumor infiltration, respectively.[81] One clinical trial found a strong relationship between [18F]DPA-714 uptake and the activation level of GAMs in patients with gliomas. They found that the expression of TSPO was mainly limited to GAMs, activated by human leukocyte antigen D-associated positivity (HLA-DR+), especially tumor-infiltrating HLA-DR+ MDSCs and TAMs, suggesting that [18F]DPA-714-PET may act as a noninvasive imaging paradigm to characterize the degree of immunosuppressive myeloid cell infiltration.[82]

Although some results have indicated that TSPO expression levels are positively correlated with the grade of malignancy, it is not clear to what extent the upregulation of TSPO reflects a proinflammatory or anti-inflammatory phenotype. Recently, Pannell *et al.* demonstrated that TSPO is explicitly upregulated in proinflammatory polarized microglia/macrophages and astrocytes after LPS and TNF stimulation, and microglia/macrophage PET imaging with the tracer 18F-DPA-713 is specific to the proinflammatory subpopulations of these cells.[114]

Third-generation TSPO receptor ligands (18F-GE-180) were subsequently produced to improve the target-background contrast. Nathalie *et al.* used this new tracer for the first time to detect the expression of TSPO in human gliomas *in vivo*. All gliomas were positive on 18F-GE-180 PET and had extraordinarily high tumor-to-background contrast. Interestingly, in the direct comparison of PET images with MRI, the highest uptake intensity could even be found in noncontrast-enhancing tumor areas, and the delineated PET volumes were larger than MRI-based tumor volumes (Figure 2(C)).[84] Furthermore, a recent clinical trial had proved that the specific uptake of 18F-GE-180 is closely related to the glioma histological WHO (World Health Organization) grade and IDH mutation status. Grade IV gliomas showed the highest uptake intensity compared with grades II and III gliomas, and IDH-WT gliomas had a higher 18F-GE-180-uptake in the overall group.[85]

In an experimental study of a mouse model of pancreatic ductal adenocarcinoma (PDAC), Lanfranca *et al.* confirmed the possibility of monitoring macrophage infiltration in the TME with the TSPO-PET tracer [11C]PBR28. There were abundant TAMs in the tumor area, and IHC and

immunofluorescence staining showed that TSPO was restricted to the surface of macrophages rather than tumor cells or other stromal cells. Autoradiography of resected tumors revealed the uptake of [11C]PBR28 by macrophages in tumors. PET imaging shows a high signal in the lung, spleen, kidney, and tumor after radiotracer injection, suggesting that [11C]PBR28 PET can serve as a valuable tool to select suitable candidates for macrophage-targeted therapies and evaluate such treatment responses.[86] Similarly, the tracer [18F]V-1008, a high-affinity TSPO-PET ligand selected by Cohen *et al.*, showed significantly increased uptake in precancerous tissue than normal pancreatic tissue, which is detectable by PET and found that [18F]V-1008 has the potential to distinguish early pancreatic cancer. However, they did not further investigate whether the increased uptake of radiotracers was due to pancreatic tumor cells or TAMs.[87] There is evidence that TSPO is preferentially expressed in activated macrophages. Nevertheless, it is not specific to M2-like TAMs and is upregulated in other stromal cells, endothelial cells, and several kinds of tumor cells.[117,118] This limits the application of TSPO tracers in specifically targeting the imaging of M2-like TAMs.

Phagocytic activity

Macrophages are an essential component of innate immunity, and serve as the first line of defense against infection. Phagocytosis is an eponymous function and remarkably stable property of the macrophage lineage. It is able to engulf various substances such as pathogens, nanoparticles, and liposomes through surface receptors and cytoplasmic recognition systems.[119,120]

At present, tracers based on the phagocytic function of macrophages are mainly used for MRI, and some involve radionuclide imaging. Scanning is usually performed 24 h after intravenous injection of the contrast agents to allow macrophages to phagocytize and infiltrate into the tumor area while allowing the unengulfed contrast agent to be cleared from the tumor. Several studies previously demonstrated that TAMs could be tracked with MRI contrast agents such as gadolinium (Gd), manganese (Mn) chelates, IONPs, and fluorine 19 (^{19}F)-incorporated perfluorocarbon compounds (PFCs).[121,122] Macrophages and Kupffer cells mainly engulf IONPS, which have been more widely used in cancer images because of their easy synthesis, high surface-to-volume

ratio, and therapeutic ability.[123,124] Ferumoxytol, a US Food and Drug Administration (FDA)–approved ultra-small superparamagnetic iron oxide (USPIO) nanoparticle, has been proven for the first time to be able to be used as a contrast agent to label TAMs by MRI in a mouse breast cancer model.[88] Recent clinical studies by Aghighi *et al.* showed that ferumoxytol tumor enhancement was noted on post-contrast scans in lymphomas and bone sarcomas of pediatric patients and young adults, especially in bone sarcomas. The decrease in MRI signal was noted to be more prominent. Moreover, the authors found that within each tumor group, $T2^{\star}$ values correlated significantly with the density of CD68+ and CD163+ TAMs on histopathology.[89] An *in vitro* study used clinical 3.0 T MRI to evaluate USPIO-MR contrast agent (P904) labeling in different macrophage populations (M0, M1, and M2) incubated with P904 for 36 h and then analyzed in gel phantoms with an MR scanner. The results showed that the M2-polarized population had a much higher T1 signal and a significantly lower $T2^{\star}$ signal than the others. Histological analysis confirmed a higher iron content in the M2-polarized population than in the M1- and M0-polarized populations.[125]

MPI is a tracer method based on tomographic imaging technology to detect the spatial distribution of superparamagnetic iron oxide (SPIO). It has the characteristics of three-dimensional imaging, high resolution and sensitivity, and no electric radiation hazard. Its signal strength is proportional to the tracer concentration and is an inspection method that can obtain quantitative data.[126] MPI has been used to detect iron-labeled TAMs in a murine model of breast cancer. In this study, the authors found that ferumoxytol (USPIO) was a superior iron nanoparticle for this application than ferucarbotran (SPIO) *in vivo*. At the same time, *in vitro* labeling of cells with the latter would provide better results. To detect and quantify macrophages in the metastatic lung environment, *ex vivo* analyses by MPI showed an increase iron in metastatic lungs at 24-h injection of USPIO *versus* control lungs, which could provide additional information that MRI could not. However, due to a large amount of iron uptake into the liver, the nanoparticle content in the lungs could not be determined *in vivo*.[90]

[19]F-based MRI is emerging as a useful tool for imaging cells. PFC nanoparticles are preferentially phagocytosed by monocytes and lack any fluorine background in the body.[127] 19F signal intensity (SI) is directly proportional to the tissue amount of the PFC, which makes ^{19}F MRI a highly sensitive and specific quantitative tool.[128] Makela *et al.* investigated *in vivo* fluorine-19 (^{19}F)-based MRI cell tracking to detect the density and distribution of TAMs and metastasis-associated macrophages (MAMs) within murine breast cancer tumors. The results showed that in the highly aggressive and metastatic four T1 tumors, the ^{19}F signal was mainly in the periphery of the tumor and in early-stage tumors, and IHC and fluorescence microscopy validated that green fluorescent F4/80 and red fluorescent PFC were observed in a similar location, indicating that ^{19}F MRI could be used to identify breast tumors with heavy infiltration of TAMs. Moreover, they showed proof of using ^{19}F MRI cell tracking to visualize MAMs in the lungs.[91] Similarly, ^{19}F MRI has been confirmed to provide a quantitative assessment of macrophage burden in tumors and sentinel lymph nodes *in vivo*. In the mouse model of head and neck squamous cell carcinoma (HNSCC), mice were subjected to MRI on days 2 and 10 after PFC injection. Cal27 tumors (double-hit, TP53 mutation combined with 3p deletion) and SCC4 tumors (single-hit, TP53 mutation alone) displayed different extents of hotspots in the periphery of the tumors, especially in Cal27 tumors. The proximal lymph nodes adjacent to the tumor were noted hotspots as well (Figure 2(D)). In *ex vivo* hematoxylin–eosin (H&E) and immunofluorescence staining analyses, the green fluorescent signal from TAMs is consistent with the MRI hotspots.[92]

Given macrophage phagocytosis imaging characteristics, the isotope for radionuclide imaging needs to have a long half-life such as ^{64}Cu ($t_{1/2} = 12.7$ h) and ^{89}Zr ($t_{1/2} = 78.4$ h). Kim *et al.* used ^{64}Cu-labeled polyglucose nanoparticles (Macrin) for quantitative PET imaging of macrophages in the TME, and found that macrophages took up Macrin with >90% selectivity by combining high-resolution *in vivo* confocal microscopy and *ex vivo* imaging of optically cleared tissue. The authors demonstrated that Macrin imaging could offer a translational method to quantify TAMs and provide therapeutic decisions.[93] Another report designed two high-yielding radiolabeling strategies to generate ^{89}Zr-HDL nanoparticles (^{89}Zr-PL-HDL and ^{89}Zr-AI-HDL), which were used to target TAMs by PET in a breast cancer model selectively. Intravenous administration of both tracers for 24-h results showed high-radioactivity accumulation in the tumor area, and *ex vivo* histologic and flow

cytometry analyses compellingly indicated TAMs as their main target.[94]

Other targets

SIGN-R1 is a calcium-dependent lectin highly expressed on macrophage surfaces.[129] Luo *et al.* developed metabolizable dextran-indocyanine green (DN-ICG) nanoprobes that selectively recognized SIGN-R1 with the second near-infrared window (NIR-II) FLI to dynamically track TAMs in subcutaneous and orthotopic mouse models of pancreatic tumors. The location of fluorescence signals of DN-ICG nanoprobes coincided perfectly with that of TAMs, indicating that this tracer could label TAMs with high sensitivity and specificity. The results showed NIR-II FLI of TAMs with high fluorescence signals in the tumor areas, liver, and spleen. Moreover, this tracer achieves a high signal-to-background ratio (SBR) in deep tissue because it can metabolize gradually in the liver but remain in pancreatic tumor stroma.[95]

TLRs are receptors of the innate immune system that recognize pathogens and are primarily expressed on macrophages and dendritic cells. TLR4 has been most closely connected to inflammation-mediated carcinogenesis and tumor progression.[130] Lee *et al.* developed anti-TLR4 antibody-ZW800-1C (TLR4-ZW800) conjugates to target TLR4 in HCC using NIRF. The groups found that this conjugate bio-distribution reflects the localization of TLR4-positive macrophages. This imaging strategy could be used to detect the increased TAM content in cancerous tissue and simultaneously evaluate the status of TLR4 signaling in solid tumors.[96] However, TLRs are also expressed on other cells, including endothelial cells, cardiac myocytes, and intestinal cells, limiting specific targeted TAM imaging.

FR-β is a cell surface receptor that is significantly upregulated on activated macrophages during inflammation but not on resting or other immune cells.[131] For this reason, it has been used as a macrophage-based therapeutic and imaging agent. For example, [Ga]Ga-NOTA-folate (Ga-FOL) was verified to be specific for targeting FR-β in a study of an atherosclerotic mouse model.[132] Another targeted FR tracer, aluminum F-labeled 1,4,7-triazacyclononane-triacetic acid conjugated folate (F-FOL), demonstrated specific uptake in inflamed myocardium containing macrophages expressing FR-β, and the nonlabeled FR-β ligand folate glucosamine could efficiently block this response *in vivo*.[133] A new contrast agent of folate-conjugated and LMW-HA-loaded ultrasonic nanobubbles (HA-FOL-NBs) was currently synthesized to target TAMs for US imaging actively, and it can reprogram TAM phenotypes from M2 to M1 as well.[97] However, targeting this receptor has been primarily used for *in vivo* imaging of activated macrophages in inflammatory diseases. Nevertheless, TAMs in the targeted TME have not been widely used, because they are expressed in specific human tumor cells, which might not be differentiated whether tracer uptake is caused specifically by cancer cells or TAMs.

F4/80, a 160-kDa cell surface glycoprotein, is highly restricted in mouse tissue macrophages. It is used as a pan-macrophage marker to detect the distribution, phenotypic heterogeneity, and activation state of TRMs. F4/80 was critical in the macrophage–NK interaction and participates in the induction of peripheral immune tolerance.[134] Terry *et al.*[98] developed ^{111}In-anti-F4/80-A3-1 and demonstrated that it could specifically bind F4/80 receptor-positive macrophages with high affinity and visualize TAMs as well as macrophages in the spleen and liver.

Given that the CSF-1R has been found to be restrictively expressed by TAMs and monocytes which more prefer to locate at the boundary of HCC. A CSF-1R-conjugated nanobubble CSF-1R (NB_{CSF-1R}) was developed using the biotinylation method and demonstrated that it might be a promising noninvasive diagnostic modality to detect the margin and residual of HCC after radiofrequency ablation (RFA).[99] In addition to the biomarkers and tracers for the *in vivo* imaging of TAMs described above, several other biomarkers have been used to detect activated macrophages in inflammatory diseases such as the macrophage scavenger receptors CD163[135] and Vsig4 (V-set and Ig domain-containing 4).[136]

Monitoring tumor immunotherapy with TAM imaging

Among the existing targeted TAM imaging methods, encouragingly, some of them have been investigated in clinical trials (Table 3). The combination of molecular imaging and tumor immunotherapy for real-time detection of the therapeutic response is the focus of clinical research. CD47 represents a promising new

Table 3. Examples of TAM-targeted imaging in clinical trials.

Target	Imaging method	Tumor type	Number of patients	Route of injection	Limitation	References
TSPO	[18F]DPA-714-PET	Glioma	9	Intravenous	Patient numbers and heterogeneity of the cohort	Zinnhardt et al.[82]
TSPO	18F-GE-180 PET	Glioma	11	Intravenous	Small sample size and the lack of histological validation	Albert et al.[84]
TSPO	18F-GE-180 PET	Glioma	58	Intravenous	The number of patients with tumor subtypes is relatively small and undergrading brain tumors at initial diagnosis	Unterrainer et al.[85]
Phagocytic activity	Ferumoxytol-MRI	Lymphoma or bone sarcoma	25	Intravenous	Calcification in tumor areas can affect the T2* signal	Aghighi et al.[89]

DPA, (N,N-diethyl-2-(2-(4-(2-fluoroethoxy)phenyl)-5,7-dimethylpyrazolo[1,5-a]pyrimidin-3-yl)acetamide; MRI, magnetic resonance imaging; PET, positron emission tomography; TAM, tumor-associated macrophage; TSPO, translocator protein.

target for osteosarcoma immunotherapy, and its mAbs have been confirmed to inhibit the interaction between CD47 and SIRPα, increasing the number of M1-like macrophages and activating phagocytes.[137–139] The Mohanty group used ferumoxytol-enhanced MRI to detect CD47 mAb therapeutic responses in osteosarcoma-bearing mice and showed significant hypo-intense (dark) ferumoxytol enhancement on post-contrast T2-MR images compared with pre-contrast images in the tumor area. CD47 mAb-treated tumors were significantly smaller than control IgG-treated tumors on day 10 of therapy. This verified the usefulness of ferumoxytol-MRI for detecting TAM response to CD47 mAb, and this imaging model is expected to be applied to monitor the therapies' response in clinical trials.[139]

Increasing evidence suggests that the TME, particularly tumor-infiltrating immune cells, including TAMs, changes significantly after radiotherapy and chemotherapy. One study used three nanoparticles, QD710-Dendron quantum dots (QD710-D), ferumoxytol, and PG-Gd-NIR813, for NIRF, T2W MRI, and dual optical/T1W MRI (Figure 3(A)) in an MDA-MB-435 tumor model. *In vivo* imaging revealed significantly higher uptake of all three nanoparticles in Abraxane-treated tumors than untreated tumors. *In vitro* studies showed that these nanoparticles were taken up by macrophages but not by tumor cells, and macrophage immunofluorescence staining and flow cytometry of single-cell suspensions from dissected tumor tissues confirmed that the infiltration of CD11b+ and CD169+ macrophages in

the tumors increased after Abraxane therapy. Moreover, NIRF optical imaging visualized increased uptake of QD710-D in Abraxane-sensitive MDA-MB-435 tumors but not in drug-resistant MDA-MB-435R tumors.[140]

By NIRF, DN-ICG has been demonstrated to target TAMs with good sensitivity and specificity. The authors further designed experiments to confirm that this imaging technique could also monitor the treatment response dynamically. Low-dose radiotherapy (5 Gy) and chemotherapy (zoledronic acid) were designed elaborately to regulate the number of TAMs in the subcutaneous model of the pancreatic tumor. They observed that the number of TAMs was twice as high as before low-dose radiotherapy (5 Gy) treatment by flow cytometry. However, after a 3-day treatment with zoledronic acid, TAMs were 50% lower than that in the control group. NIRF analysis of TAMs revealed that the fluorescence signal in the tumor region increased twofold in the low-dose radiotherapy group and decreased by 50% in the zoledronic acid-treated group at 6, 12, and 24 h after the injection of DN-ICG (Figure 3(B)), which was consistent with the flow cytometric analysis.[95] These studies indicate that noninvasive imaging techniques can observe the quantitative changes in TAMs and assess the early treatment response using imageable nanoparticles.

Discussion and conclusion
Given the crucial roles of TAMs in orchestrating tumor progression, preclinical and clinical
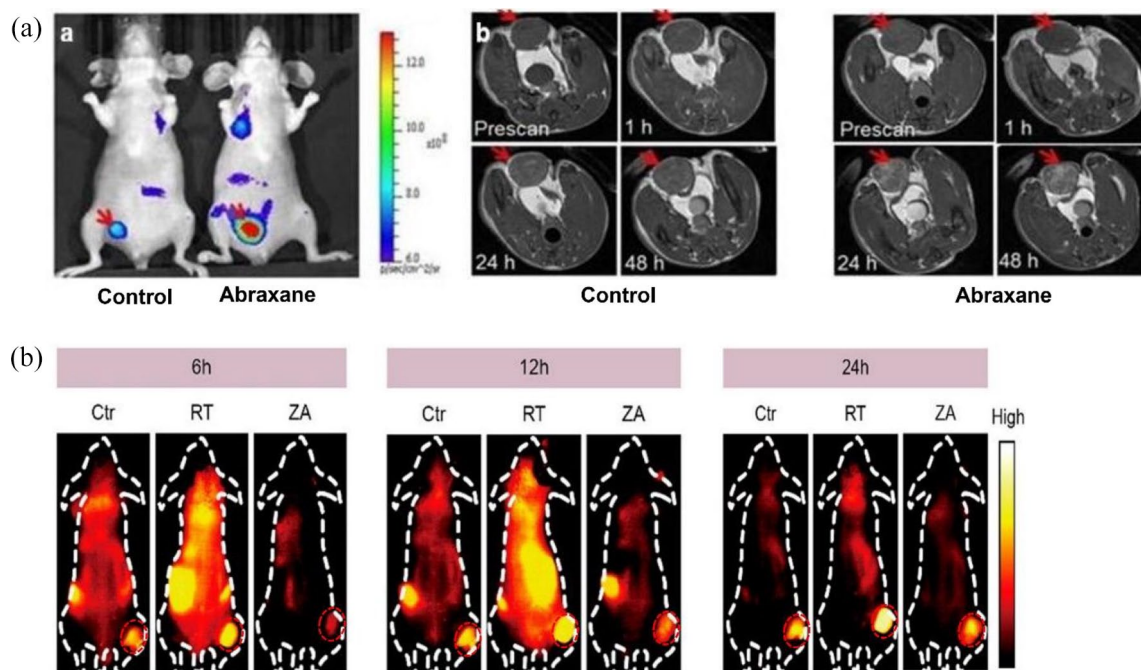
Figure 3. Monitoring immunotherapy by molecular imaging of TAMs. (A) Optical imaging and T1W MRI *in vivo* response to Abraxane treatment of MDA-MB-435 tumor. (a) NIRF image MDA-MB-435 tumors at 48 h after injection of PG-Gd-NIR813. (b) T1W MRI of MDA-MB-435 tumors before and 1, 24, and 48 h after injection of PG-Gd-NIR813. Adapted with permission from Cao *et al.*[140] (B) *In vivo* NIR-II fluorescence imaging of DN-ICG response to low-dose radiotherapy and chemotherapy in the subcutaneous model of the pancreatic tumor. *In vivo* NIR-II fluorescence imaging of DN-ICG was intravenously injected in different groups, and images were acquired after 6, 12, and 24 h, respectively (ICG dose = 0.5 mg/kg). Adapted with permission from Luo *et al.*[95] with minor modifications.
Ctr, control (without treatment); RT, radiotherapy (5 Gy X-ray); ZA: zoledronic acid.

trials have demonstrated that targeting TAMs is a novel and promising approach to improving antitumor therapy. The classification, distribution, and density of TAMs in the TME vary among individuals and tumor types and change dynamically during treatment. There is an urgent need to have an accurate understanding of TAMs in the TME. This review shows that molecular imaging techniques can provide better means for the noninvasive, real-time, and quantitative *in vivo* tracking of TAMs, contributing to selecting suitable patients before immunotherapy, and potentially guide clinical treatment decisions. Further imaging studies are needed to explore new tracers that can deliberately target M1 macrophages and make full use of the advantages of different imaging techniques to improve the accuracy, specificity, and sensitivity of macrophage targeting. Moreover, TAM-targeted diagnostic probes could be coupled with therapeutic drugs to realize individualized treatment guided by real-time dynamic images.

Author contributions

Xiaoying Li: Conceptualization; Supervision; Validation; Writing – original draft; Writing – review & editing.

Ruike Wang: Conceptualization; Software; Writing – original draft.

Yangnan Zhang: Conceptualization; Formal analysis; Writing – original draft.

Shuangze Han: Conceptualization; Software; Writing – original draft.

Yu Gan: Conceptualization; Software.

Qi Liang: Visualization.

Xiaoqian Ma: Conceptualization; Visualization.

Pengfei Rong: Conceptualization; Funding acquisition; Supervision; Validation; Writing – original draft; Writing – review & editing.

Wei Wang: Funding acquisition; Supervision; Validation; Writing – original draft; Writing – review & editing.

Wei Li: Conceptualization; Funding acquisition; Supervision; Validation; Writing – original draft; Writing – review & editing.

ORCID iDs
Xiaoying Li https://orcid.org/0000-0001-6541-064X

Wei Li https://orcid.org/0000-0002-7267-6494

References

1. Gangadaran P and Ahn BC. Molecular imaging: a useful tool for the development of natural killer cell-based immunotherapies. *Front Immunol* 2017; 8: 1090. DOI: 10.3389/fimmu.2017.01090.

2. Palmer AE and Hammond MC. Editorial overview: molecular imaging. *Curr Opin Chem Biol* 2020; 57: A5–A7. DOI: 10.1016/j.cbpa.2020.07.002.

3. Dammes N and Peer D. Monoclonal antibody-based molecular imaging strategies and theranostic opportunities. *Theranostics* 2020; 10: 938–955. DOI: 10.7150/thno.37443.

4. Blasberg RG and Gelovani-Tjuvajev J. In vivo molecular-genetic imaging. *J Cell Biochem Suppl* 2002; 39: 172–183. DOI: 10.1002/jcb.10433.

5. Youn H and Hong KJ. In vivo noninvasive small animal molecular imaging. *Osong Public Health Res Perspect* 2012; 3: 48–59. DOI: 10.1016/j.phrp.2012.02.002.

6. Florea A, Mottaghy FM and Bauwens M. Molecular imaging of angiogenesis in oncology: current preclinical and clinical status. *Int J Mol Sci* 2021; 22: 5544. DOI: 10.3390/ijms22115544.

7. Bonnet S, Prévot G, Mornet S, *et al*. A nano-emulsion platform functionalized with a fully human scFv-Fc antibody for atheroma targeting: towards a theranostic approach to atherosclerosis. *Int J Mol Sci* 2021; 22: 5188. DOI: 10.3390/ijms22105188.

8. Coda AR, Anzilotti S, Boscia F, *et al*. In vivo imaging of CNS microglial activation/macrophage infiltration with combined [(18)F] DPA-714-PET and SPIO-MRI in a mouse model of relapsing remitting experimental autoimmune encephalomyelitis. *Eur J Nucl Med Mol Imaging* 2021; 48: 40–52. DOI: 10.1007/s00259-020-04842-7.

9. Hanahan D and Weinberg RA. Hallmarks of cancer: the next generation. *Cell* 2011; 144: 646–674. DOI: 10.1016/j.cell.2011.02.013.

10. Barlesi F and Tomasini P. Non-small-cell lung cancer brain metastases and PD-(L)1 immune checkpoint inhibitors. *Lancet Oncol* 2020; 21: 607–608. DOI: 10.1016/S1470-2045(20)30207-2.

11. Herrscher H and Robert C. Immune checkpoint inhibitors in melanoma in the metastatic, neoadjuvant, and adjuvant setting. *Curr Opin Oncol* 2020; 32: 106–113. DOI: 10.1097/CCO.0000000000000610.

12. Zhang Y, Hughes KR, Raghani RM, *et al*. Cargo-free immunomodulatory nanoparticles combined with anti-PD-1 antibody for treating metastatic breast cancer. *Biomaterials* 2021; 269: 120666. DOI: 10.1016/j.biomaterials.2021.120666.

13. Zou F, Tan J, Liu T, *et al*. The CD39(+) HBV surface protein-targeted CAR-T and personalized tumor-reactive CD8(+) T cells exhibit potent anti-HCC activity. *Mol Ther* 2021; 29: 1794–1807. DOI: 10.1016/j.ymthe.2021.01.021.

14. Zins K and Abraham D. Cancer immunotherapy: targeting tumor-associated macrophages by gene silencing. *Methods Mol Biol* 2020; 2115: 289–325. DOI: 10.1007/978-1-0716-0290-4_17.

15. Mantovani A, Marchesi F, Malesci A, *et al*. Tumour-associated macrophages as treatment targets in oncology. *Nat Rev Clin Oncol* 2017; 14: 399–416. DOI: 10.1038/nrclinonc.2016.217.

16. Qian BZ and Pollard JW. Macrophage diversity enhances tumor progression and metastasis. *Cell* 2010; 141: 39–51. DOI: 10.1016/j.cell.2010.03.014.

17. Meng YM, Sun J, Qv N, *et al*. Application of molecular imaging technology in tumor immunotherapy. *Cell Immunol* 2020; 348: 104039.

18. Wang Y, Lin YX, Qiao SL, *et al*. Progress in tumor-associated macrophages: from bench to bedside. *Adv Biosyst* 2019; 3: e1800232. DOI: 10.1002/adbi.201800232.

19. Movahedi K, Laoui D, Gysemans C, *et al.* Different tumor microenvironments contain functionally distinct subsets of macrophages derived from Ly6C(high) monocytes. *Cancer Res* 2010; 70: 5728–5739. DOI: 10.1158/0008-5472. CAN-09-4672.

20. Li X, Liu R, Su X, *et al.* Harnessing tumor-associated macrophages as aids for cancer immunotherapy. *Mol Cancer* 2019; 18: 177. DOI: 10.1186/s12943-019-1102-3.

21. Albini A, Bruno A, Noonan DM, *et al.* Contribution to tumor angiogenesis from innate immune cells within the tumor microenvironment: implications for immunotherapy. *Front Immunol* 2018; 9: 527. DOI: 10.3389/fimmu.2018.00527.

22. Salmaninejad A, Valilou SF, Soltani A, *et al.* Tumor-associated macrophages: role in cancer development and therapeutic implications. *Cell Oncol (Dordr)* 2019; 42: 591–608. DOI: 10.1007/s13402-019-00453-z.

23. Kim J and Bae JS. Tumor-associated macrophages and neutrophils in tumor microenvironment. *Mediators Inflamm* 2016; 2016: 6058147. DOI: 10.1155/2016/6058147.

24. Nie G, Cao X, Mao Y, *et al.* Tumor-associated macrophages-mediated CXCL8 infiltration enhances breast cancer metastasis: suppression by Danirixin. *Int Immunopharmacol* 2021; 95: 107153. DOI: 10.1016/j.intimp.2020.107153.

25. Sun D, Luo T, Dong P, *et al.* M2-polarized tumor-associated macrophages promote epithelial-mesenchymal transition via activation of the AKT3/PRAS40 signaling pathway in intrahepatic cholangiocarcinoma. *J Cell Biochem* 2020; 121: 2828–2838. DOI: 10.1002/jcb.29514.

26. Murray PJ, Allen JE, Biswas SK, *et al.* Macrophage activation and polarization: nomenclature and experimental guidelines. *Immunity* 2014; 41: 14–20. DOI: 10.1016/j.immuni.2014.06.008.

27. Ruffell B and Coussens LM. Macrophages and therapeutic resistance in cancer. *Cancer Cell* 2015; 27: 462–472. DOI: 10.1016/j.ccell.2015.02.015.

28. Chen Y, Jin H, Song Y, *et al.* Targeting tumor-associated macrophages: a potential treatment for solid tumors. *J Cell Physiol* 2021; 236: 3445–3465. DOI: 10.1002/jcp.30139.

29. van Dalen FJ, van Stevendaal M, Fennemann FL, *et al.* Molecular repolarisation of tumour-associated macrophages. *Molecules* 2018; 24: 9. DOI: 10.3390/molecules24010009.

30. Guerriero JL. Macrophages: the road less traveled, changing anticancer therapy. *Trends* *Mol Med* 2018; 24: 472–489. DOI: 10.1016/j.molmed.2018.03.006.

31. Magkouta SF, Vaitsi PC, Pappas AG, *et al.* CSF1/CSF1R axis blockade limits mesothelioma and enhances efficiency of anti-PDL1 immunotherapy. *Cancers* 2021; 13: 2546. DOI: 10.3390/cancers13112546.

32. Wang Y, Tiruthani K, Li S, *et al.* mRNA delivery of a bispecific single-domain antibody to polarize tumor-associated macrophages and synergize immunotherapy against liver malignancies. *Adv Mater* 2021; 33: 2007603. DOI: 10.1002/adma.202007603.

33. Dammeijer F, Lievense LA, Kaijen-Lambers ME, *et al.* Depletion of tumor-associated macrophages with a CSF-1R kinase inhibitor enhances antitumor immunity and survival induced by DC immunotherapy. *Cancer Immunol Res* 2017; 5: 535–546. DOI: 10.1158/2326-6066.CIR-16-0309.

34. Li K, Xu W, Lu K, *et al.* CSF-1R inhibition disrupts the dialog between leukaemia cells and macrophages and delays leukaemia progression. *J Cell Mol Med* 2020; 24: 13115–13128. DOI: 10.1111/jcmm.15916.

35. Kitamura T, Qian BZ, Soong D, *et al.* CCL2-induced chemokine cascade promotes breast cancer metastasis by enhancing retention of metastasis-associated macrophages. *J Exp Med* 2015; 212: 1043–1059. DOI: 10.1084/jem.20141836.

36. Moisan F, Francisco EB, Brozovic A, *et al.* Enhancement of paclitaxel and carboplatin therapies by CCL2 blockade in ovarian cancers. *Mol Oncol* 2014; 8: 1231–1239. DOI: 10.1016/j.molonc.2014.03.016.

37. Yang Z, Li H, Wang W, *et al.* CCL2/CCR2 axis promotes the progression of salivary adenoid cystic carcinoma via recruiting and reprogramming the tumor-associated macrophages. *Front Oncol* 2019; 9: 231. DOI: 10.3389/fonc.2019.00231.

38. Felsenstein M, Blank A, Bungert AD, *et al.* CCR2 of tumor microenvironmental cells is a relevant modulator of glioma biology. *Cancers* 2020; 12: 1882. DOI: 10.3390/cancers12071882.

39. Song J-S, Chang C-C, Wu C-H, *et al.* A highly selective and potent CXCR4 antagonist for hepatocellular carcinoma treatment. *Proc Natl Acad Sci U S A* 2021; 118: e2015433118. DOI: 10.1073/pnas.2015433118.

40. Zhou W, Ke SQ, Huang Z, *et al.* Periostin secreted by glioblastoma stem cells recruits M2 tumour-associated macrophages and promotes

malignant growth. *Nat Cell Biol* 2015; 17: 170–182. DOI: 10.1038/ncb3090.

41. Casagrande N, Borghese C, Favero A, *et al.* Trabectedin overcomes doxorubicin-resistance, counteracts tumor-immunosuppressive reprogramming of monocytes and decreases xenograft growth in Hodgkin lymphoma. *Cancer Lett* 2021; 500: 182–193. DOI: 10.1016/j. canlet.2020.12.015.

42. Van Acker HH, Anguille S, Willemen Y, *et al.* Bisphosphonates for cancer treatment: mechanisms of action and lessons from clinical trials. *Pharmacol Ther* 2016; 158: 24–40. DOI: 10.1016/j.pharmthera.2015.11.008.

43. Zhang Q, Le K, Xu M, *et al.* Combined MEK inhibition and tumor-associated macrophages depletion suppresses tumor growth in a triple-negative breast cancer mouse model. *Int Immunopharmacol* 2019; 76: 105864. DOI: 10.1016/j.intimp.2019.105864.

44. Zang X, Zhang X, Hu H, *et al.* Targeted delivery of zoledronate to tumor-associated macrophages for cancer immunotherapy. *Mol Pharmaceut* 2019; 16: 2249–2258. DOI: 10.1021/acs. molpharmaceut.9b00261.

45. Scott EM, Jacobus EJ, Lyons B, *et al.* Bi- and tri-valent T cell engagers deplete tumour-associated macrophages in cancer patient samples. *J Immunother Cancer* 2019; 7: 320. DOI: 10.1186/ s40425-019-0807-6.

46. Rodriguez PL, Harada T, Christian DA, *et al.* Minimal 'self' peptides that inhibit phagocytic clearance and enhance delivery of nanoparticles. *Science (New York, NY)* 2013; 339: 971–975. DOI: 10.1126/science.1229568.

47. Veillette A and Chen J. SIRPα-CD47 immune checkpoint blockade in anticancer therapy. *Trends Immunol* 2018; 39: 173–184. DOI: 10.1016/j. it.2017.12.005.

48. Zhang W, Huang Q, Xiao W, *et al.* Advances in anti-tumor treatments targeting the CD47/SIRPα axis. *Front Immunol* 2020; 11: 18. DOI: 10.3389/ fimmu.2020.00018.

49. Petrova PS, Viller NN, Wong M, *et al.* TTI-621 (SIRPαFc): a CD47-blocking innate immune checkpoint inhibitor with broad antitumor activity and minimal erythrocyte binding. *Clin Cancer Res* 2017; 23: 1068–1079. DOI: 10.1158/1078-0432. CCR-16-1700.

50. Hutter G, Theruvath J, Graef CM, *et al.* Microglia are effector cells of CD47-SIRPα antiphagocytic axis disruption against glioblastoma. *Proc Natl Acad Sci U S A* 2019; 116: 997–1006. DOI: 10.1073/pnas.1721434116.

51. Sikic BI, Lakhani N, Patnaik A, *et al.* First-in-human, first-in-class phase I trial of the anti-CD47 antibody Hu5F9-G4 in patients with advanced cancers. *J Clin Oncol* 2019; 37: 946–953. DOI: 10.1200/JCO.18.02018.

52. Singha AK, Sarkar C, Majumder D, *et al.* IL-15 and GM-CSF stimulated macrophages enhances phagocytic activity in ENU induced leukemic mice. *Immunobiology* 2020; 225: 151894. DOI: 10.1016/j.imbio.2019.12.003.

53. Hardie J, Mas-Rosario JA, Ha S, *et al.* Macrophage activation by a substituted pyrimido[5,4-b]indole increases anti-cancer activity. *Pharmacol Res* 2019; 148: 104452. DOI: 10.1016/j.phrs.2019.104452.

54. Maeda A, Digifico E, Andon FT, *et al.* Poly(I:C) stimulation is superior than Imiquimod to induce the antitumoral functional profile of tumor-conditioned macrophages. *Eur J Immunol* 2019; 49: 801–811. DOI: 10.1002/eji.201847888.

55. Fujiwara T, Yakoub MA, Chandler A, *et al.* CSF-1/CSF-1R signaling inhibitor pexidartinib (PLX3397) reprograms tumor-associated macrophages and stimulates T-cell infiltration in the sarcoma microenvironment. *Mol Cancer Ther* 2021; 20: 1388–1399. DOI: 10.1158/1535-7163. MCT-20-0591.

56. Wang L, Hu Y-Y, Zhao J-L, *et al.* Targeted delivery of miR-99b reprograms tumor-associated macrophage phenotype leading to tumor regression. *J Immunother Cancer* 2020; 8: e000517. DOI: 10.1136/jitc-2019-000517.

57. Wang Y-C, Wang X, Yu J, *et al.* Targeting monoamine oxidase A-regulated tumor-associated macrophage polarization for cancer immunotherapy. *Nat Commun* 2021; 12: 3530. DOI: 10.1038/s41467-021-23164-2.

58. Vonderheide RH. CD40 agonist antibodies in cancer immunotherapy. *Annu Rev Med* 2020; 71: 47–58. DOI: 10.1146/annurev-med-062518-045435.

59. Cassetta L and Pollard JW. Targeting macrophages: therapeutic approaches in cancer. *Nat Rev Drug Discov* 2018; 17: 887–904. DOI: 10.1038/nrd.2018.169.

60. Shan H, Dou W, Zhang Y, *et al.* Targeted ferritin nanoparticle encapsulating CpG oligodeoxynucleotides induces tumor-associated macrophage M2 phenotype polarization into M1 phenotype and inhibits tumor growth. *Nanoscale* 2020; 12: 22268–22280. DOI: 10.1039/ d0nr04520a.

61. Zhao J-L, Huang F, He F, *et al.* Forced activation of notch in macrophages represses tumor growth

by upregulating miR-125a and disabling tumor-associated macrophages. *Cancer Res* 2016; 76: 1403–1415. DOI: 10.1158/0008-5472.CAN-15-2019.

62. Wiehagen KR, Girgis NM, Yamada DH, *et al.* Combination of CD40 agonism and CSF-1R blockade reconditions tumor-associated macrophages and drives potent antitumor immunity. *Cancer Immunol Res* 2017; 5: 1109–1121. DOI: 10.1158/2326-6066.CIR-17-0258.

63. Beatty GL, Torigian DA, Chiorean EG, *et al.* A phase I study of an agonist CD40 monoclonal antibody (CP-870,893) in combination with gemcitabine in patients with advanced pancreatic ductal adenocarcinoma. *Clin Cancer Res* 2013; 19: 6286–6295. DOI: 10.1158/1078-0432.CCR-13-1320.

64. Du Y, Jin Y, Sun W, *et al.* Advances in molecular imaging of immune checkpoint targets in malignancies: current and future prospect. *Eur Radiol* 2019; 29: 4294–4302. DOI: 10.1007/s00330-018-5814-3.

65. Ametamey SM, Honer M and Schubiger PA. Molecular imaging with PET. *Chem Rev* 2008; 108: 1501–1516. DOI: 10.1021/cr0782426.

66. Pichler BJ, Judenhofer MS and Pfannenberg C. Multimodal imaging approaches: PET/CT and PET/MRI. *Handb Exp Pharmacol* 2008; 185: 109–132. DOI: 10.1007/978-3-540-72718-7_6.

67. Lu ZR. Magnetic resonance molecular imaging for non-invasive precision cancer diagnosis. *Curr Opin Biomed Eng* 2017; 3: 67–73. DOI: 10.1016/j.cobme.2017.11.003.

68. Serkova NJ, Glunde K, Haney CR, *et al.* Preclinical applications of multi-platform imaging in animal models of cancer. *Cancer Res* 2021; 81: 1189–1200. DOI: 10.1158/0008-5472.CAN-20-0373.

69. Coatney RW. Ultrasound imaging: principles and applications in rodent research. *ILAR J* 2001; 42: 233–247.

70. La Fleur L, Botling J, He F, *et al.* Targeting MARCO and IL37R on immunosuppressive macrophages in lung cancer blocks regulatory T cells and supports cytotoxic lymphocyte function. *Cancer Res* 2021; 81: 956–967. DOI: 10.1158/0008-5472.CAN-20-1885.

71. Wang W, Gao Z, Wang L, *et al.* Application and prospects of molecular imaging in immunotherapy. *Cancer Manag Res* 2020; 12: 9389–9403. DOI: 10.2147/CMAR.S269773.

72. Movahedi K, Schoonooghe S, Laoui D, *et al.* Nanobody-based targeting of the macrophage mannose receptor for effective in vivo imaging of tumor-associated macrophages. *Cancer Res* 2012; 72: 4165–4177. DOI: 10.1158/0008-5472.CAN-11-2994.

73. Locke LW, Mayo MW, Yoo AD, *et al.* PET imaging of tumor associated macrophages using mannose coated 64Cu liposomes. *Biomaterials* 2012; 33: 7785–7793. DOI: 10.1016/j.biomaterials.2012.07.022.

74. Blykers A, Schoonooghe S, Xavier C, *et al.* PET imaging of macrophage mannose receptor-expressing macrophages in tumor stroma using 18F-radiolabeled camelid single-domain antibody fragments. *J Nucl Med* 2015; 56: 1265–1271. DOI: 10.2967/jnumed.115.156828.

75. Zhang C, Yu X, Gao L, *et al.* Noninvasive imaging of CD206-positive M2 macrophages as an early biomarker for post-chemotherapy tumor relapse and lymph node metastasis. *Theranostics* 2017; 7: 4276–4288.

76. Xavier C, Blykers A, Laoui D, *et al.* Clinical translation of [(68)Ga]Ga-NOTA-anti-MMR-sdAb for PET/CT imaging of protumorigenic macrophages. *Mol Imaging Biol* 2019; 21: 898–906. DOI: 10.1007/s11307-018-01302-5.

77. Zhang C, Gao L, Cai Y, *et al.* Inhibition of tumor growth and metastasis by photoimmunotherapy targeting tumor-associated macrophage in a sorafenib-resistant tumor model. *Biomaterials* 2016; 84: 1–12. DOI: 10.1016/j.biomaterials.2016.01.027.

78. Jiang C, Cai H, Peng X, *et al.* Targeted imaging of tumor-associated macrophages by cyanine 7-labeled mannose in xenograft tumors. *Mol Imaging* 2017; 16: 1536012116689499. DOI: 10.1177/1536012116689499.

79. Sun X, Gao D, Gao L, *et al.* Molecular imaging of tumor-infiltrating macrophages in a preclinical mouse model of breast cancer. *Theranostics* 2015; 5: 597–608. DOI: 10.7150/thno.11546.

80. Li YC, Wu H, Ji B, *et al.* Targeted imaging of CD206 expressing tumor-associated M2-like macrophages using mannose-conjugated antibiofouling magnetic iron oxide nanoparticles. *ACS Appl Bio Mater* 2020; 3: 4335–4347. DOI: 10.1021/acsabm.0c00368.

81. Pigeon H, Peres EA, Truillet C, *et al.* TSPO-PET and diffusion-weighted MRI for imaging a mouse model of infiltrative human glioma. *Neuro Oncol* 2019; 21: 755–764. DOI: 10.1093/neuonc/noz029.

82. Zinnhardt B, Müther M, Roll W, *et al.* TSPO imaging-guided characterization of the immunosuppressive myeloid tumor microenvironment in patients with malignant

glioma. *Neuro Oncol* 2020; 22: 1030–1043. DOI: 10.1093/neuonc/noaa023.

83. Buck JR, McKinley ET, Fu A, *et al.* Preclinical TSPO ligand PET to visualize human glioma xenotransplants: a preliminary study. *PLoS ONE* 2015; 10: e0141659. DOI: 10.1371/journal.pone.0141659.

84. Albert NL, Unterrainer M, Fleischmann DF, *et al.* TSPO PET for glioma imaging using the novel ligand (18)F-GE-180: first results in patients with glioblastoma. *Eur J Nucl Med Mol Imaging* 2017; 44: 2230–2238.

85. Unterrainer M, Fleischmann DF, Vettermann F, *et al.* TSPO PET, tumour grading and molecular genetics in histologically verified glioma: a correlative F-GE-180 PET study. *Eur J Nucl Med Mol I* 2020; 47: 1368–1380. DOI: 10.1007/s00259-019-04491-5.

86. Lanfranca MP, Lazarus J, Shao X, *et al.* Tracking macrophage infiltration in a mouse model of pancreatic cancer with the positron emission tomography tracer [11C]PBR28. *J Surg Res* 2018; 232: 570–577.

87. Cohen AS, Li J, Hight MR, *et al.* TSPO-targeted PET and optical probes for the detection and localization of premalignant and malignant pancreatic lesions. *Clin Cancer Res* 2020; 26: 5914–5925. DOI: 10.1158/1078-0432.CCR-20-1214.

88. Daldrup-Link HE, Golovko D, Ruffell B, *et al.* MRI of tumor-associated macrophages with clinically applicable iron oxide nanoparticles. *Clin Cancer Res* 2011; 17: 5695–5704. DOI: 10.1158/1078-0432.CCR-10-3420.

89. Aghighi M, Theruvath AJ, Pareek A, *et al.* Magnetic resonance imaging of tumor-associated macrophages: clinical translation. *Clin Cancer Res* 2018; 24: 4110–4118. DOI: 10.1158/1078-0432.CCR-18-0673.

90. Makela AV, Gaudet JM, Schott MA, *et al.* Magnetic particle imaging of macrophages associated with cancer: filling the voids left by iron-based magnetic resonance imaging. *Mol Imaging Biol* 2020; 22: 958–968. DOI: 10.1007/s11307-020-01473-0.

91. Makela AV and Foster PJ. Imaging macrophage distribution and density in mammary tumors and lung metastases using fluorine-19 MRI cell tracking. *Magn Reson Med* 2018; 80: 1138–1147. DOI: 10.1002/mrm.27081.

92. Khurana A, Chapelin F, Xu HY, *et al.* Visualization of macrophage recruitment in head and neck carcinoma model using fluorine-19 magnetic resonance imaging. *Magn Reson Med* 2018; 79: 1972–1980. DOI: 10.1002/mrm.26854.

93. Kim HY, Li R, Ng TSC, *et al.* Quantitative imaging of tumor-associated macrophages and their response to therapy using (64)Cu-labeled Macrin. *ACS Nano* 2018; 12: 12015–12029. DOI: 10.1021/acsnano.8b04338.

94. Perez-Medina C, Tang J, Abdel-Atti D, *et al.* PET imaging of tumor-associated macrophages with 89Zr-labeled high-density lipoprotein nanoparticles. *J Nucl Med* 2015; 56: 1272–1277. DOI: 10.2967/jnumed.115.158956.

95. Luo X, Hu D, Gao D, *et al.* Metabolizable near-infrared-II nanoprobes for dynamic imaging of deep-seated tumor-associated macrophages in pancreatic cancer. *ACS Nano* 2021; 15: 10010–10024. DOI: 10.1021/acsnano.1c01608.

96. Ji Y, Wang Z, Bao K, *et al.* Targeted molecular imaging of TLR4 in hepatocellular carcinoma using zwitterionic near-infrared fluorophores. *Quant Imaging Med Surg* 2019; 9: 1548–1555. DOI: 10.21037/qims.2019.09.04.

97. Sun X, Guo L, Shang M, *et al.* Ultrasound mediated destruction of LMW-HA-Loaded and folate-conjugated nanobubble for TAM targeting and reeducation. *Int J Nanomedicine* 2020; 15: 1967–1981. DOI: 10.2147/IJN.S238587.

98. Terry SYA, Boerman OC, Gerrits D, *et al.* ^{111}In-anti-F4/80-A3-1 antibody: a novel tracer to image macrophages. *Eur J Nucl Med Mol Imaging* 2015; 42: 1430–1438. DOI: 10.1007/s00259-015-3084-8.

99. Jiang QC, Zeng YT, Xu YN, *et al.* Ultrasound molecular imaging as a potential non-invasive diagnosis to detect the margin of hepatocarcinoma via CSF-1R targeting. *Front Bioeng Biotechnol* 2020; 8: 783. DOI: 10.3389/fbioe.2020.00783.

100. Martinez-Pomares L. The mannose receptor. *J Leukocyte Biol* 2012; 92: 1177–1186. DOI: 10.1189/jlb.0512231.

101. Liu DR, Guan QL, Gao MT, *et al.* Mannose receptor as a potential biomarker for gastric cancer: a pilot study. *Int J Biol Marker* 2017; 32: E278–E283. DOI: 10.5301/jbm.5000244.

102. Arteta B, Lasuen N, Lopategi A, *et al.* Colon carcinoma cell interaction with liver sinusoidal endothelium inhibits organ-specific antitumor immunity through interleukin-1-induced mannose receptor in mice. *Hepatology* 2010; 51: 2172–2182. DOI: 10.1002/hep.23590.

103. Maupin KA, Sinha A, Eugster E, *et al.* Glycogene expression alterations associated with pancreatic cancer epithelial-mesenchymal transition in complementary model systems.

PLoS ONE 2010; 5: e13002. DOI: 10.1371/journal.pone.0013002.

104. Keyaerts M, Xavier C, Heemskerk J, *et al.* Phase I study of 68Ga-HER2-nanobody for PET/CT assessment of HER2 expression in breast carcinoma. *J Nucl Med* 2016; 57: 27–33. DOI: 10.2967/jnumed.115.162024.

105. Azad AK, Rajaram MVS, Metz WL, *et al.* γ-Tilmanocept, a new radiopharmaceutical tracer for cancer sentinel lymph nodes, binds to the mannose receptor (CD206). *J Immunol* 2015; 195: 2019–2029. DOI: 10.4049/jimmunol.1402005.

106. Varasteh Z, Mohanta S, Li Y, *et al.* Targeting mannose receptor expression on macrophages in atherosclerotic plaques of apolipoprotein E-knockout mice using 68Ga-NOTA-anti-MMR nanobody: non-invasive imaging of atherosclerotic plaques. *EJNMMI Res* 2019; 9: 5. DOI: 10.1186/s13550-019-0474-0.

107. Toribio RE, Young N, Schlesinger LS, *et al.* Cy3-tilmanocept labeling of macrophages in joints of mice with antibody-induced arthritis and synovium of human patients with rheumatoid arthritis. *J Orthop Res* 2021; 39: 821–830. DOI: 10.1002/jor.24900.

108. Coda AR, Anzilotti S, Boscia F, *et al.* In vivo imaging of CNS microglial activation/macrophage infiltration with combined [F]DPA-714-PET and SPIO-MRI in a mouse model of relapsing remitting experimental autoimmune encephalomyelitis. *Eur J Nucl Med Mol I* 2021; 48: 40–52. DOI: 10.1007/s00259-020-04842-7.

109. Lavisse S, Goutal S, Wimberley C, *et al.* Increased microglial activation in patients with Parkinson disease using [18F]-DPA714 TSPO PET imaging. *Parkinsonism Relat Disord* 2021; 82: 29–36. DOI: 10.1016/j.parkreldis.2020.11.011.

110. Vlodavsky E and Soustiel JF. Immunohistochemical expression of peripheral benzodiazepine receptors in human astrocytomas and its correlation with grade of malignancy, proliferation, apoptosis and survival. *J Neurooncol* 2007; 81: 1–7.

111. Veenman L, Levin E, Weisinger G, *et al.* Peripheral-type benzodiazepine receptor density and in vitro tumorigenicity of glioma cell lines. *Biochem Pharmacol* 2004; 68: 689–698. DOI: 10.1016/j.bcp.2004.05.011.

112. Junck L, Olson JM, Ciliax BJ, *et al.* PET imaging of human gliomas with ligands for the peripheral benzodiazepine binding site. *Ann Neurol* 1989; 26: 752–758.

113. Pappata S, Cornu P, Samson Y, *et al.* PET study of carbon-11-PK 11195 binding to peripheral type benzodiazepine sites in glioblastoma: a case report. *J Nucl Med* 1991; 32: 1608–1610.

114. Pannell M, Economopoulos V, Wilson TC, *et al.* Imaging of translocator protein upregulation is selective for pro-inflammatory polarized astrocytes and microglia. *Glia* 2020; 68: 280–297.

115. Winkeler A, Boisgard R, Awde AR, *et al.* The translocator protein ligand [18F]DPA-714 images glioma and activated microglia in vivo. *Eur J Nucl Med Mol Imaging* 2012; 39: 811–823. DOI: 10.1007/s00259-011-2041-4.

116. Zinnhardt B, Pigeon H, Thézé B, *et al.* Combined PET imaging of the inflammatory tumor microenvironment identifies margins of unique radiotracer uptake. *Cancer Res* 2017; 77: 1831–1841.

117. Narayan N, Owen DR, Mandhair H, *et al.* Translocator protein as an imaging marker of macrophage and stromal activation in rheumatoid arthritis pannus. *J Nucl Med* 2018; 59: 1125–1132. DOI: 10.2967/jnumed.117.202200.

118. Batarseh A and Papadopoulos V. Regulation of translocator protein 18 kDa (TSPO) expression in health and disease states. *Mol Cell Endocrinol* 2010; 327: 1–12. DOI: 10.1016/j.mce.2010.06.013.

119. Gordon S. Phagocytosis: an immunobiologic process. *Immunity* 2016; 44: 463–475. DOI: 10.1016/j.immuni.2016.02.026.

120. Locati M, Curtale G and Mantovani A. Diversity, mechanisms, and significance of macrophage plasticity. *Annu Rev Pathol* 2020; 15: 123–147. DOI: 10.1146/annurev-pathmechdis-012418-012718.

121. Tan M, Wu X, Jeong EK, *et al.* An effective targeted nanoglobular manganese(II) chelate conjugate for magnetic resonance molecular imaging of tumor extracellular matrix. *Mol Pharm* 2010; 7: 936–943. DOI: 10.1021/mp100054m.

122. Yang R, Sarkar S, Yong VW, *et al.* In vivo MR imaging of tumor-associated macrophages: the next frontier in cancer imaging. *Magn Reson Insights* 2018; 11: 1178623X18771974. DOI: 10.1177/1178623X18771974.

123. Ansari C, Tikhomirov GA, Hong SH, *et al.* Development of novel tumor-targeted theranostic nanoparticles activated by membrane-type matrix metalloproteinases for combined cancer magnetic resonance imaging

and therapy. *Small* 2014; 10: 566–575. DOI: 10.1002/smll.201301456.

124. Dadfar SM, Roemhild K, Drude NI, *et al*. Iron oxide nanoparticles: diagnostic, therapeutic and theranostic applications. *Adv Drug Deliv Rev* 2019; 138: 302–325. DOI: 10.1016/j.addr.2019.01.005.

125. Zini C, Venneri MA, Miglietta S, *et al*. USPIO-labeling in M1 and M2-polarized macrophages: an in vitro study using a clinical magnetic resonance scanner. *J Cell Physiol* 2018; 233: 5823–5828. DOI: 10.1002/jcp.26360.

126. Panagiotopoulos N, Duschka RL, Ahlborg M, *et al*. Magnetic particle imaging: current developments and future directions. *Int J Nanomedicine* 2015; 10: 3097–3114. DOI: 10.2147/IJN.S70488.

127. Temme S, Jacoby C, Ding Z, *et al*. Technical advance: monitoring the trafficking of neutrophil granulocytes and monocytes during the course of tissue inflammation by noninvasive 19F MRI. *J Leukoc Biol* 2014; 95: 689–697. DOI: 10.1189/jlb.0113032.

128. Flogel U, Ding Z, Hardung H, *et al*. In vivo monitoring of inflammation after cardiac and cerebral ischemia by fluorine magnetic resonance imaging. *Circulation* 2008; 118: 140–148. DOI: 10.1161/CIRCULATIONAHA.107.737890.

129. Anthony RM, Wermeling F, Karlsson MCI, *et al*. Identification of a receptor required for the anti-inflammatory activity of IVIG. *Proc Natl Acad Sci U S A* 2008; 105: 19571–19578. DOI: 10.1073/pnas.0810163105.

130. Liu C-Y, Xu J-Y, Shi X-Y, *et al*. M2-polarized tumor-associated macrophages promoted epithelial-mesenchymal transition in pancreatic cancer cells, partially through TLR4/IL-10 signaling pathway. *Lab Invest* 2013; 93: 844–854. DOI: 10.1038/labinvest.2013.69.

131. Jager NA, Westra J, Golestani R, *et al*. Folate receptor-β imaging using 99mTc-folate to explore distribution of polarized macrophage populations in human atherosclerotic plaque. *J Nucl Med* 2014; 55: 1945–1951. DOI: 10.2967/jnumed.114.143180.

132. Moisio O, Palani S, Virta J, *et al*. Radiosynthesis and preclinical evaluation of [Ga]Ga-NOTA-folate for PET imaging of folate receptor β-positive macrophages. *Sci Rep* 2020; 10: 13593. DOI: 10.1038/s41598-020-70394-3.

133. Jahandideh A, Uotila S, Ståhle M, *et al*. Folate receptor β-targeted PET imaging of macrophages in autoimmune myocarditis. *J Nucl Med* 2020; 61: 1643–1649. DOI: 10.2967/jnumed.119.241356.

134. Lin H-H, Stacey M, Stein-Streilein J, *et al*. F4/80: the macrophage-specific adhesion-GPCR and its role in immunoregulation. *Adv Exp Med Biol* 2010; 706: 149–156.

135. Eichendorff S, Svendsen P, Bender D, *et al*. Biodistribution and PET imaging of a novel [68Ga]-anti-CD163-antibody conjugate in rats with collagen-induced arthritis and in controls. *Mol Imaging Biol* 2015; 17: 87–93. DOI: 10.1007/s11307-014-0768-6.

136. Zheng F, Luo S, Ouyang Z, *et al*. NIRF-molecular imaging with synovial macrophages-targeting Vsig4 nanobody for disease monitoring in a mouse model of arthritis. *Int J Mol Sci* 2019; 20: 3347. DOI: 10.3390/ijms20133347.

137. Edris B, Weiskopf K, Volkmer AK, *et al*. Antibody therapy targeting the CD47 protein is effective in a model of aggressive metastatic leiomyosarcoma. *Proc Natl Acad Sci U S A* 2012; 109: 6656–6661. DOI: 10.1073/pnas.1121629109.

138. Zhao XW, van Beek EM, Schornagel K, *et al*. CD47-signal regulatory protein-alpha (SIRPalpha) interactions form a barrier for antibody-mediated tumor cell destruction. *Proc Natl Acad Sci U S A* 2011; 108: 18342–18347. DOI: 10.1073/pnas.1106550108.

139. Mohanty S, Yerneni K, Theruvath JL, *et al*. Nanoparticle enhanced MRI can monitor macrophage response to CD47 mAb immunotherapy in osteosarcoma. *Cell Death Dis* 2019; 10: 36. DOI: 10.1038/s41419-018-1285-3.

140. Cao Q, Yan X, Chen K, *et al*. Macrophages as a potential tumor-microenvironment target for noninvasive imaging of early response to anticancer therapy. *Biomaterials* 2018; 152: 63–76. DOI: 10.1016/j.biomaterials.2017.10.036.

Visit SAGE journals online
journals.sagepub.com/home/tam

Ⓢ SAGE journals